Asian Journal of Chemistry; Vol. 34, No. 4 (2022), 959-966

ASIAN JOURNAL OF CHEMISTRY

https://doi.org/10.14233/ajchem.2022.23625

Mononuclear Manganese(IV) Complexes Derived from Polyfunctional Fumaryldihydrazone

P. MAHANTA[1], P. SARMA[1], D. BASUMATARY[1,*] and C. MEDHI[2]

[1]Department of Applied Sciences, Gauhati University, Guwahati-781014, India
[2]Department of Chemistry, Gauhati University, Guwahati-781014, India

*Corresponding author: E-mail: debbasumatary@gmail.com; debbasumatary@gauhati.ac.in

Received: 22 November 2021; *Accepted*: 15 January 2022; *Published online*: 10 March 2022; AJC-20740

A series of mononuclear manganese(IV) complexes of disalicylaldehyde fumaroyldihydrazone ($slfhH_4$) were synthesized by reacting manganese acetate tetrahydrate with dihydrazone in absence and presence of various pyridine bases in methanol medium. Pyridine (py) and its derivatives like 2-picoline (2-pic), 3-picoline (3-pic), 4-picoline (4-pic), 2,2′-bipyridine (bpy) and 1,10-phenanthroline (phen) were added to the reaction mixture of metal salt and dihydrazone to explore the binding possibilities of these molecules to manganese center. The elemental analysis, mass spectral and thermal studies were used to derive their composition. Study of magnetic moment, molar conductances, electronic, EPR and infrared spectroscopy have led to interpretation of their tentative structures. Magnetic moment and EPR studies correspond to their Mn(IV) oxidation state. The dihydrazone functions as tetradentate ligand chelating the manganese(IV) ion present in octahedral geometry with anti-*cis* configuration in enol form. Electrochemical and antimicrobial studies were also performed.

Keywords: Disalicylaldehyde fumaroyldihydrazone, Manganese(IV), Octahedral stereochemistry, Antimicrobial studies.

INTRODUCTION

The synthesis of a novel ligand is perhaps the most essential step in the growth of metal complexes which exhibit distinctive properties. Since, the electron donor and electron acceptor properties of the ligands, structural, functional groups and the position of the ligand in the coordination sphere together with the reactivity of coordination compounds may be the factor for different studies [1,2]. Correspondingly, hydrazone as ligands can create an environment similar to biological systems by usually making coordination through oxygen and nitrogen atoms. Hydrazone derivatives possessing anti-inflammatory, analgesic [3], antipyretic [4], antibacterial [5] and antitumor [6] activities are also reported in the literature. In last two decades, polyfunctional dihydrazones have developed as an interesting field of investigation to many researchers [7,8]. Their versatility is rendered due to their flexibility, chelation, easy synthesis and applications have widened their prospective in research.

Acyl, aroyl- or pyridoyl dihydrazines on condensation with *o*-hydroxy aromatic aldehydes and ketones form dihydrazones that possess up to four oxygen and four nitrogen atoms as donors [9], which are available as bonding sites to same or different metal atoms [10-12]. Hence, they are likely to yield complexes of stable nature with many transition metal ions [12]. The hydrazones have wide field of applications pertaining to areas like organic, inorganic, medicinal and analytical chemistry [13,14]. Present work focuses in the coordination chemistry of disalicylaldehyde fumaroyldihydrazone and its manganese complexes. This work stems from the fact that only a few hydrazone derived complexes of manganese are known and reported. Few of these reports for manganese complexes show their potential application as biomimetics for enzymes [15,16]. In general, manganese is known to play several key roles in biological processes [15]. It has been known to facilitate an important role in water oxidation and evolution of oxygen in photosynthetic systems [17] and also has stimulated profound interest in the various fields of catalysis and photochemistry [18,19]. Manganese in the +2 oxidation state has dominated the coordination chemistry of manganese and comparatively few manganese complexes in +4 oxidation state have been documented [15,20,21]. We herein present a notably electron-rich dihydrazone as a ligand which can stabilize the manganese in a high oxidation state in the isolated stable complexes. Also to the best of our knowledge, work

with the title dihydrazone and its manganese complexes are not yet reported and hence the following work is of immense interest and so has been carried out.

EXPERIMENTAL

The chemicals *viz*. $Mn(OAc)_2{\cdot}4H_2O$, hydrazine hydrate ($N_2H_4{\cdot}H_2O$), salicylaldehyde, diethyl fumarate, ethanol and methanol were of analytical grade reagents.

Standard procedure was followed to determine manganese [22]. Manganese(IV) complexes in DMSO (10^{-3} M) were prepared and their molar conductances were measured using direct reading conductivitymeter-304 with a dip-type conductivity cell at room temperature. Microanalytical data of carbon, hydrogen and nitrogen were collected using Euro EA elemental analyser. Magnetic susceptibility were measured on a Sherwood Scientific Magnetic Susceptibility Balance with $Hg[Co(SCN)_4]$ as the calibrating agent at room temperature. Infrared spectral data were obtained using Spectrum 2 Perkin-Elmer FTIR spectrometer from 4000-500 cm^{-1} in KBr disks. EPR spectral data of the complexes as powders and in DMSO were measured on JES-FA200 ESR spectrometer with X-band frequency at room temperature (RT) and liquid nitrogen temperature (LNT). LC-MS spectra of complexes were obtained from UHPLC-ULTIMATE 3000, Thermoscientific, MS-Exactive Plus spectrometer. Electronic spectral data were obtained within the range 250 to 800 nm in DMSO on a Perkin-Elmer Lambda 35 UV-Vis spectrophotometer. Melting point and decomposition temperatures were obtained using Analab melting apparatus, μ Thermocal 10. Thermal stability and decomposition of the analytical complexes were determined by means of Mettler Toledo thermal analyser system recording TGA and DTG curves in the temperature range 25-700 ºC under N_2 atmosphere with a heating rate of 20 ºC min^{-1}. Electrochemical studies for complexes in DMSO were carried under pure and dry dinitrogen atmosphere using CHI660D CH Instrument electrochemical work station with Pt disk as working electrode, a Pt wire auxiliary electrode and a Ag/AgCl reference electrode.

Synthesis of ligand ($slfhH_4$): Ligand disalicylaldehyde fumaroyldihydrazone was prepared in two steps. In first step, fumaric dihydrazide was obtained by reacting diethyl fumarate (6.95 g, 40.36 mmol) with hydrazine hydrate (3.07 g, 61 mmol) in 1:2 molar ratio in ethanol. In second step, fumaric dihydrazide obtained above was added with salicylaldehyde (0.244 g, 2 mmol) in 1:2 molar ratio under reflux for 1 h in ethanol. A yellow precipitate was obtained that was washed several times with hot methanol and dried over anhydrous $CaCl_2$ (decomp. temp. 250 ºC).

Synthesis of complex 1: $Mn(OAc)_2{\cdot}4H_2O$ (0.24g, 1 mmol) in methanol (15 mL) was added to a methanolic solution (15 mL) of ligand ($slfhH_4$) (0.31 g, 1 mmol) at 1:1 molar ratio. The mixture was stirred at room temperature for 15 min and then refluxed for 2 h. An orange coloured product was obtained that was filtered, washed with hot methanol and dried over anhydrous $CaCl_2$ (yield: 68%).

Synthesis of complexes 1-7: The above method was essentially followed for the synthesis of manganese(IV) complexes proceeded by the addition of pyridine bases to the reaction mixture of $Mn(OAc)_2{\cdot}4H_2O$ and $slfhH_4$ in methanol solution maintaining $Mn(OAc)_2{\cdot}4H_2O$:$slfhH_4$:pyridine at a molar ratio of 1:1:10 for pyridine bases and 1:1:2 in case of 2,2′-bipyridine and 1,10-phenanthroline [yield: 64% (**2**), (**3**); 64% (**4**), (**5**); 62% (**6**) and 57 % (**7**)] (**Scheme-I**).

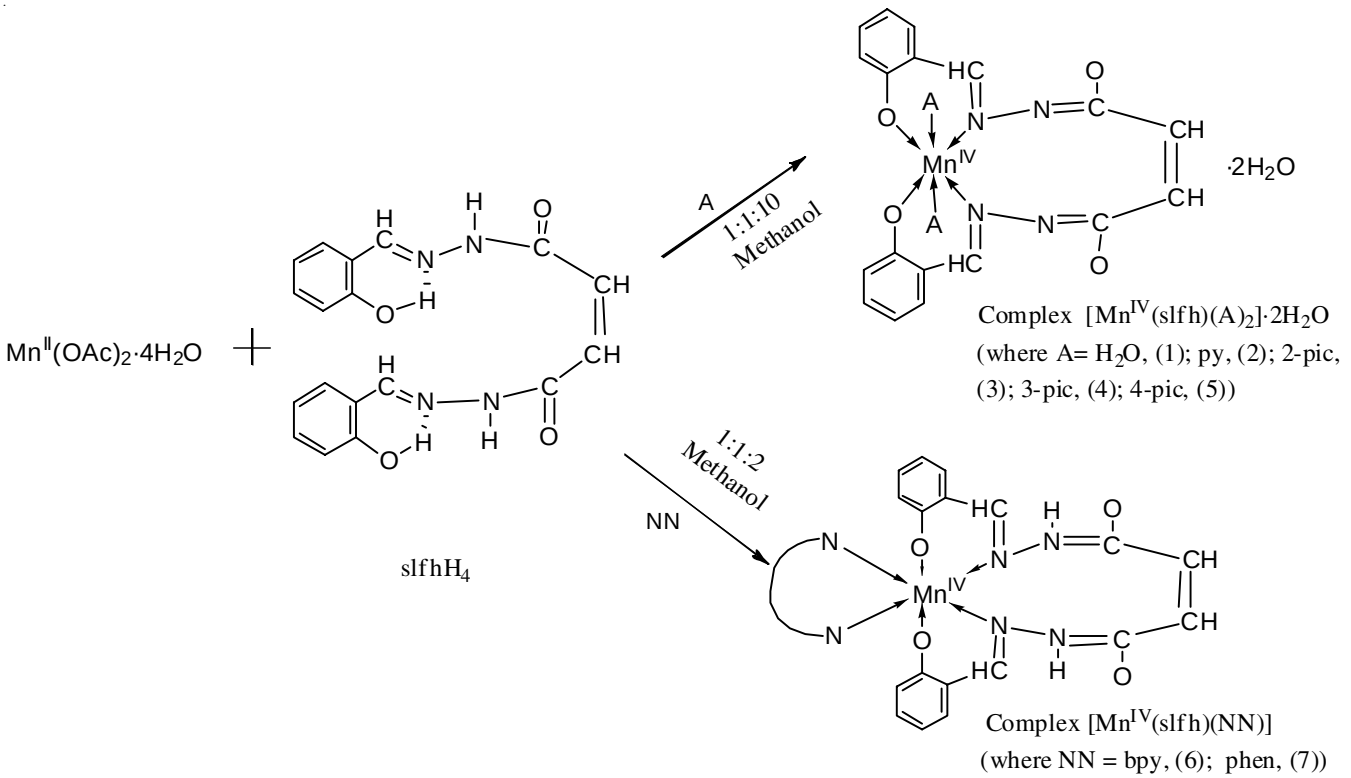

Scheme-I: Reaction and structure of the Mn(IV) complexes

Antimicrobial susceptibility tests: The standard agar well diffusion method [23,24] was followed while evaluating the *in vitro* antibacterial properties of the ligand and its Mn(IV) complexes while taking into consideration the bacteria *viz. Staphylococcus epidermis* (MTCC 435), *Bacillus cereus* (MTCC 1305), *Klebsiella pneumonia* (MTCC 10309), *Escherichia coli* (MTCC 1669), *Enterobacter aerogenes* (MTCC 8559) and *Proteus vulgaris* (MTCC 426). Complexes **1**, **2**, **3**, **4** and **7** were allowed to diffuse through the agar gel previously inoculated with a test bacterial pathogen. After incubation of the plates for 24-48 h, the bacterial colonies showed a growth wherever possible and produced a haze in the agar. The microorganism served as parameter, for visibility and activity of the complexes. In order to ascertain that the antimicrobial activity was not due to the solvent, 5% DMSO solvent, was also tested as negative control.

RESULTS AND DISCUSSION

All the Mn(IV) complexes are stable in air and insoluble in water and common organic solvents. However, they are completely soluble in DMSO and DMF. The analytical data along with their colour, decomposition point, and molar conductance are presented in Table-1. The ligand and its Mn(IV) complexes decompose above 250 ºC. Complexes **1-5** show weight loss at 110 ºC that indicates the presence of water molecules being present in the lattice structure. The extent of weight loss at 180 ºC relates to the loss of two molecules of water present in coordination to the metal center for complex **1**. Also, the weight loss at 220 ºC in complexes **2**-**7** correspond to the expulsion of two pyridine or a substituted pyridine molecule in the case of complexes **6** and **7**, the weight loss at this temperature corresponds to the expulsion of only one bipyridine or 1,10-phenanthroline molecule.

Unfortunately, the formation of only amorphous solids even after several efforts for crystallization prevented use of X-ray crystallography to confirm the molecularity and the proposed structures of these complexes.

Thermal studies: The complexes do not decompose or melt up to the observed temperature range of 250 ºC that reveal strong metal-ligand bonds with higher ionic character. The thermogravimetric analysis had been conducted considering the complexes **1** and **2** as representative samples. Complex **1** within the temperature range of 29-118 ºC and corresponding DTG peak at 59 ºC exhibited degradation as observed in the TGA/DTG curve. The corresponding weight loss of 7.59% (calcd. 8.15%) have been assumed to be due to the loss of weight by two lattice water molecules. The degradation in the second stage within the temperature range of 120-192 ºC with DTG peak at 171 ºC and weight loss of 2.06% (calcd. 2.10%) corresponds to the discharge of half coordinated water molecules. In the third stage degradation within the temperature range of 196-292 ºC with DTG peak at 248 ºC and weight loss of 2.10% (calcd.1.73%) corresponds to the liberation of half coordinated water molecule and organic moiety ($-C_2H_2$). A weight loss of 10.46% (calcd. 11.12%) in the fourth degradation stage within the temperature range, 300-366 ºC corresponds to the discharge of half coordinated water molecule and organic moiety ($-C_2H_2$) with associated DTG peak is observed at 356 ºC. The liberation of organic moiety ($-COCON_2$) with DTG peak at 409 ºC in the fifth stage exhibited one degradation observed between 370-458 ºC with a weight loss of 22.29% (calcd. 23.46%). The sixth degradation stage showed weight loss of 9.22% (calcd. 9.53%) that occurred between 474-592 ºC is associated with the DTG curve is observed at 538 ºC attributed to the loss of (-CHN) moiety. The overall weight loss have been found to be 53.72% as against the calculated value of 56.09%. The disintegration of complex **2** exhibited five stages of degradation as revealed by the TGA curve. Details for the stages of thermal decomposition and the percentage loss of masses along with their assigned molecules/fragments are summarized in Table-2. The curve of complex **2** that is displayed as representative complex in Fig. 1. These thermal investigations indicated the presence of two water molecules in the lattice of complexes **1** and **2** and also two coordinated water molecules in the structure of complex **1**, which are in good agreement with their IR spectral studies [25,26].

Molar conductance: The molar conductance values of the synthesized complexes are given in Table-1. The values lie in the range 0.70-1.3 ohm^{-1} cm^2 mol^{-1} in DMSO solution that indicate they are non-electrolytes [10,11,21].

Mass spectrum: Ligand and complex **1** were characterized by LC-MS spectroscopy as representative samples. The signal observed at *m/z* 350 in the mass spectrum of ligand is attributable to $[slfhH_2]^+$ species. A signal at *m/z* 402 in complex 1 may have resulted from the formation of $[Mn(slfh)]^+$ fragment. The signal due to the formation of such species in the mass spectrum of the complex indicates that the complex is monomeric in nature.

TABLE-1
COLOUR, DECOMPOSITION POINT, ANALYTICAL, MAGNETIC MOMENT AND MOLAR CONDUCTANCE DATA OF Mn(IV) COMPLEXES OF $slfhH_4$

Complex	Colour	D.P. (°C)	Elemental analysis (%): Found (calcd.)				μ_B (B.M.)	Molar conductance (Λ_m) (ohm^{-1} cm^2 mol^{-1})
			Mn	C	H	N		
$[Mn(slfh)(H_2O)_2]\cdot 2H_2O$	Orange	> 250	11.94 (12.58)	49.01 (49.42)	2.95 (3.20)	11.99 (12.81)	4.12	0.79
$[Mn(slfh)(py)_2]\cdot 2H_2O$	Dark orange	> 250	9.04 (9.80)	59.22 (59.89)	3.40 (3.92)	14.54 (14.97)	3.68	0.86
$[Mn(slfh)(2\text{-}pic)_2]\cdot 2H_2O$	Dark orange	> 250	8.87 (9.83)	60.65 (61.12)	3.89 (4.41)	13.79 (14.26)	3.80	0.83
$[Mn(slfh)(3\text{-}pic)_2]\cdot 2H_2O$	Dark orange	> 250	9.21 (9.83)	59.95 (61.12)	4.12 (4.41)	13.89 (14.26)	4.02	0.98
$[Mn(slfh)(4\text{-}pic)_2]\cdot 2H_2O$	Dark orange	> 250	9.01 (9.83)	60.05 (61.12)	3.95 (4.14)	14.04 (14.26)	4.11	1.30
[Mn(slfh)(bpy)]	Pale orange	> 250	9.11 (9.84)	58.99 (60.10)	3.17 (3.57)	14.65 (15.02)	4.02	0.90
[Mn(slfh)(phen)]	Pale orange	> 250	9.18 (9.43)	60.13 (61.74)	3.02 (3.43)	13.97 (14.40)	4.11	0.70

TABLE-2
THERMOANALYTICAL RESULTS (TG AND DTG) FOR MANGANESE(IV) COMPLEXES OF LIGAND DISALICYLALDEHYDE FUMARYLDIHYDRAZONE

Complexes	TG range (°C)	DTG (°C)	Found (calcd.) (%)		Assignment
			Mass loss	Total mass loss	
$[Mn(slfh)(H_2O)_2]\cdot 2H_2O$ (**1**)	29-118	59	7.59 (8.15)	53.72 (56.09)	Loss of two lattice H_2O molecule
	120-192	171	2.06 (2.10)		Loss of half coordinated H_2O molecule
	196-292	248	2.10 (1.73)		Loss of half coordinated H_2O molecule
	300-366	356	10.46 (11.12)		Loss of half coordinated water molecule and organic moiety ($-C_2H_2$)
	370-458	409	22.29 (23.46)		Loss of organic moiety ($-COCON_2$)
	474-592	538	9.22 (9.53)		Loss of organic moiety (-CHN)
$[Mn(slfh)(py)_2]\cdot 2H_2O$ (**2**)	29-110	62	6.05 (7.17)	54.47 (55.12)	Loss of two lattice H_2O molecule
	130-288	262	4.65 (4.69)		Loss of organic moiety ($-C_2H_2$)
	292-335	320	12.92 (12.16)		Loss of organic moiety ($CHCON_2$)
	342-475	405	23.02 (22.89)		Loss of one pyridine base molecule & N_2
	475-596	533	7.83 (8.21)		Loss of organic moiety (-CO)

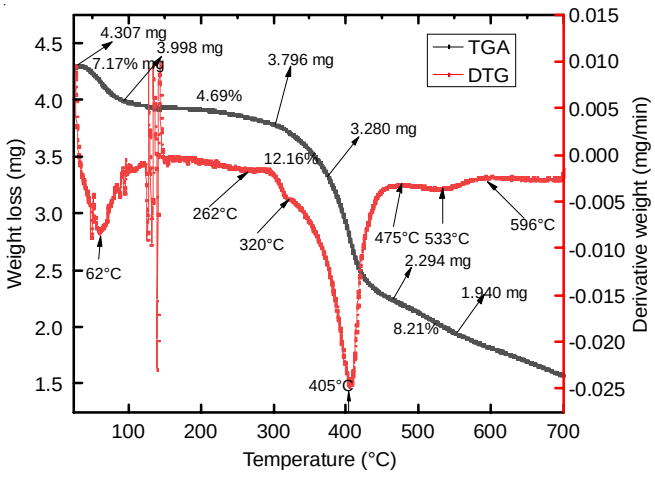

Fig. 1. TGA and DTG curves of $[Mn^{IV}(slfh)(py)_2]\cdot 2H_2O$ (**2**)

Magnetic moment: The μ_B values fall in the range 3.68-4.12 B.M. and are listed in Table-1. These values are characteristic of manganese(IV) complexes in a d^3 high spin electronic configuration without any spin-spin coupling between unpaired electrons of neighboring Mn(IV) centers in the structural unit of solids at room temperature [15,20,21].

Electronic spectra: The electronic spectral bands for dihydrazone and its manganese(IV) complexes along with their molar extinction coefficients are shown in Table-3. The spectra of the complexes are shown in Fig. 2. The absorption spectrum of free ligand is characterized by weak absorption band at 314 nm and a strong band at 352 nm with molar extin-ction coefficients of 3587 and 5990 $dm^3\ mol^{-1}\ cm^{-1}$, respectively. These spectral bands arise from intraligand π-π* and n-π* transitions. Complexes **1** and **6** show one intraligand weak band at 295 and 292 nm, respectively. However, in other complexes, this weak intra-ligand band disappear or is merged with another prominent band with a blue shift of 1-23 nm in these compl-exes. New bands appear in the region 430-483 nm in all these complexes. These features in the spectra of complexes indicate chelation of dihydrazone to manganese center. Octahedral Mn(IV) complexes are usually expected to show three spin allowed *d-d* transitions. The absorption bands in 430-483 nm region may be attributed to *d-d* transition, $^4A_{2g} \rightarrow {}^4T_{2g}$ in the manganese(IV) complexes. However, their high molar extinction coefficients appear to have large contribution from ligand-to-metal charge transfer [21,27]. Other two *d-d* transition bands expected are obscured either by ligand or charge transfer bands in the region.

EPR spectra: The relevant EPR parameters of the Mn(IV) complexes are listed in Table-3. The spectra of the complexes are similar to one another in the polycrystalline phase at room temperature. The isotropic signal has a g-value in the range 2.032-2.045 and no other signal is visible. However, in DMSO at RT and LNT, six hyperfine lines are observed with hyperfine splitting constant between 80-100 G range for complexes

TABLE-3
IMPORTANT ELECTRONIC SPECTRAL BANDS AND EPR DATA FOR MANGANESE(IV) COMPLEXES OF LIGAND DISALICYLALDEHYDEFUMARYLDIHYDRAZONE

Ligand/Complex	λ_{max}, nm (ε_{max}, $dm^3\ mol^{-1}\ cm^{-1}$)	Temperature	Solid/Solution	g-value	A_{Mn} (G)
$slfhH_4$	314 (3587), 352 (5990)	–	–	–	–
$[Mn(slfh)(H_2O)_2]\cdot 2H_2O$	295 (6340), 348 (2330), 442 (2113)	LNT	DMSO	2.036	80
		RT	DMSO	1.940	100
		RT	Solid	2.045	–
$[Mn(slfh)(py)_2]\cdot 2H_2O$	346 (5433), 434 (2684)	RT	Solid	2.045	–
$[Mn(slfh)(2\text{-}pic)_2]\cdot 2H_2O$	351 (8290), 483 (6525)	RT	Solid	2.032	–
$[Mn(slfh)(3\text{-}pic)_2]\cdot 2H_2O$	332 (5882), 430 (4473)	LNT	DMSO	2.033	100
		RT	DMSO	1.970	100
$[Mn(slfh)(4\text{-}pic)_2]\cdot 2H_2O$	333 (5882), 430 (4431)	–	–	–	–
[Mn(slfh)(bpy)	292 (4142), 346 (4709), 435 (3152)	RT	Solid	2.045	–
[Mn(slfh)(phen)]	330 (5531), 431 (4650)	RT	Solid	2.045	–

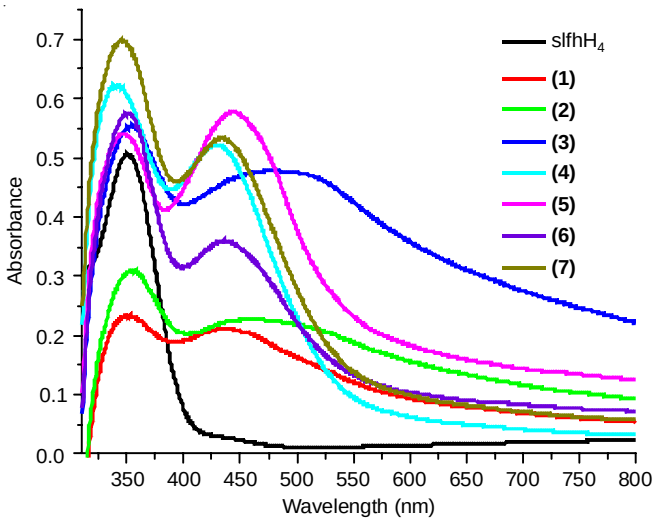

Fig. 2. Electronic spectra of ligand slfhH$_4$ and complexes [Mn^{IV}(slfh)(H$_2$O)$_2$]·2H$_2$O (**1**), [Mn^{IV}(slfh)(py)$_2$]·2H$_2$O (**2**), [Mn^{IV}(slfh)(2-pic)$_2$]·2H$_2$O (**3**), [Mn^{IV}(slfh)(3-pic)$_2$]·2H$_2$O (**4**), [Mn^{IV}(slfh)(4-pic)$_2$]·2H$_2$O (**5**), [Mn^{IV}(slfh)(phen)] (**6**), [Mn^{IV}(slfh)(bpy)] (**7**)

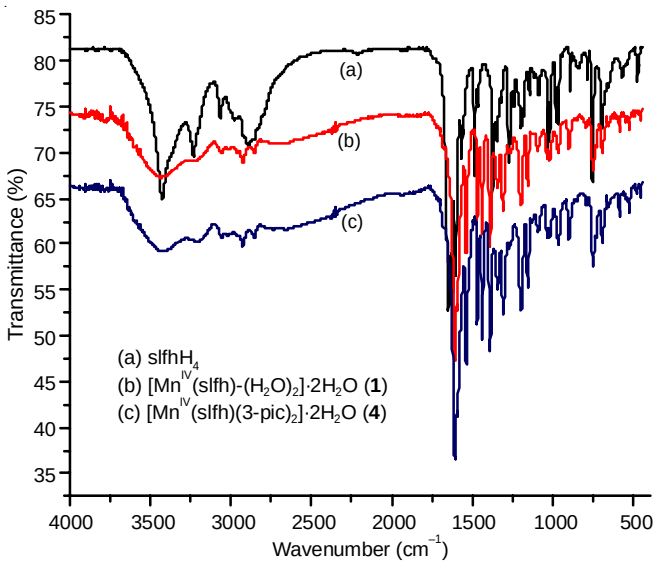

Fig. 3. Infrared spectra of ligand (a) slfhH$_4$ and complexes (b) [Mn^{IV}(slfh)-(H$_2$O)$_2$]·2H$_2$O (**1**) (c) [Mn^{IV}(slfh)(3-pic)$_2$]·2H$_2$O (**4**)

1 and **4** [21]. These ^{55}Mn hyperfine splitting constant is close to that usually observed for Mn(IV) complexes. The signal due to ^{55}Mn hyperfine splitting is weak for complex **1** in DMSO at LNT. Further, superhyperfine lines are observable for complex **4** at LNT in DMSO. The characteristic features of the spectra relates to Mn(IV) being present in pseudo-octahedral environment.

Infrared spectra: Structurally key IR spectral bands for dihydrazone and its complexes are presented in Table-4 and the IR spectra of free dihydrazone, complexes **1** and **4** are presented in Fig. 3. The ligand shows medium to strong bands in the region centered at 3424, 3229 and 3066 cm^{-1} that are assigned to the stretching vibrations of phenolic -OH and *sec.* -NH group [22]. In the synthesized complexes, above bands are replaced by broad bands in the region between 3600-3000 cm^{-1}. The appearance of such feature indicates the disappearance of -NH group on complexation [21]. The bands in this region are observed due to the existence of stretching vibration of phenolic -OH group or due to the presence of coordinated/lattice water molecules. Further, the ν(NH) band at 3229 cm^{-1} in free dihydrazone is absent in IR spectra of complexes. The dihydrazone shows a strong ν(C=O) band at 1648 cm^{-1}, which is absent in complexes indicating destruction of amide structure and coordination of ligand to the metal center in enol form. The IR spectrum of ligand shows two strong bands at 1623 and 1604 cm^{-1} attributed to stretching vibration due to azomethine groups. These bands shift to a lower frequency by an average of 11-17 cm^{-1} in the complexes [20,28]. The appearance of ν(C=N) stretching vibration as two bands in IR spectra of complexes like in free dihydrazone suggests that the two >C=N groups are in equivalent. This arises from the coordination of

TABLE-4
STRUCTURALLY SIGNIFICANT IR SPECTRAL BANDS OF DISALICYLALDEHYDE FUMAROYLDIHYDRAZONE AND ITS MONOMETALLIC MANGANESE(IV) COMPLEXES

Ligand/ Complex	ν[(OH) + (NH)]	ν(C=O)	ν(C=N)	ν[Amide(II) + (CO) phenolic	ν(C-O) phenolic	ν(N-N)	ν(M-O) phenolic	ν(M-N) py/bpy/phen vibration in-plane
slfhH$_4$	3000-3600(sbr) 3424(s) 3229(s) 3066(m)	1648(s)	1623(s) 1604(s)	1564(s)	1273(s) 1244(m)	1035(s) 1017(s)	–	–
1	3000-3600(sbr) 3410(s)	–	1613(s) 1592(s)	1543(s)	1271(w)	1044(s)	586(m)	–
2	3000-3600(mbr) 3420(m)	–	1613(s) 1591(s)	1543(s)	1264(w)	1037(m)	586(m)	651(w)
3	3000-3600(mbr) 3440(mbr)	–	1612(s) 1591(s)	1543(s)	1270(w)	1042(w)	585(w)	652(w)
4	3000-3600(mbr) 3410(m)	–	1602(s) 1592(s)	1532(s)	1269(w)	1038(m)	585(m)	654(w)
5	3000-3600(mbr) 3410(m)	–	1602(vs) 1592(s)	1543(s)	1286(m)	1042(w)	585(m)	655(w)
6	3000-3600(mbr) 3390(m)	–	1602(s) 1592(s)	1543(m)	1286(m)	1042(w)	585(w)	655(w)
7	3000-3650(mbr) 3424(m))	–	1608(s) 1593(s)	1537(s)	1271(w)	1039(m)	588(w)	654(w)

dihydrazone to the same metal centre, which results in generation of anti-*cis* configuration where one hydrazone arm occupies axial position while the other hydrazone arm occupies equatorial position around the metal center. The two bands of strong and moderate intensities at 1273 and 1244 cm^{-1}, respectively are assigned to β(C-O)(phenolic) in free dihydrazone. These bands in ligand appear as single band in complexes and shift to higher frequency by 5-27 cm^{-1} on an average and is suggested that the phenolic C-O group is involved in coordination to the metal centre. Non-ligand bands of medium to weak intensity are observed in the region 588-585 cm^{-1}, which are tentatively assigned to ν(M-O)(phenolic) band that indicate flow of π-electron density from aromatic ring to metal center through phenolic oxygen atoms [29]. The IR spectral band at 604 cm^{-1} is attributable to absorption due to free pyridine bases as a result of in-plane ring deformation. A new medium to weak band in complexes in the region 655-651 cm^{-1} are assigned to in-plane ring deformation of pyridine bases suggesting their coordination to the metal center [30]. The strong broad band centered at 3410 cm^{-1} in complex **1** indicates the presence of coordinated water molecules [21] and the lattice water molecules while the broad band in the region 3600-3000 cm^{-1} in the complexes **2-5** appears to have a contribution from a lattice water molecules.

Cyclic voltammetry studies: The cyclic voltammetric (CV) data are shown in Table-5 at a scan rate of 100 mV/s and the cyclic voltammogram of the ligand $slfhH_4$ and complex **2** are presented in Fig. 4. The CV analysis of ligand and complexes **1**, **2** and **3** were performed with 2 mmol solution in DMSO using 0.1 mol L^{-1} TBAP as a supporting electrolyte under dinitrogen atmosphere. The free ligand exhibits two quasi-reversible redox couples at +0.38 V ($E_{1/2}$) (ΔE = 240 mV) and 0.99 V ($E_{1/2}$) (ΔE = 80 mV) and an irreversible anodic peak potential at +0.83 V against Ag/AgCl. The voltammograms of complexes showed oxidative and reductive peaks of ligand, which appear slightly shifted or almost unshifted from their original position in ligand. These features suggested the presence of ligand-based redox activity. However, these complexes do not show manganese centered redox peaks [29,31].

TABLE-5
ELECTROCHEMICAL DATA FOR MANGANESE(IV) COMPLEXES (POTENTIAL *vs.* Ag/AgCl)

Ligand/Complex	Anodic potential, E_{pa} (V)	Cathodic potential, E_{pc} (V)
$slfhH_4$	-0.26	-0.50
	+0.83	–
	+1.03	+ 0.95
$[Mn(slfh)(H_2O)_2]\cdot 2H_2O$ (**1**)	-0.26	-0.50
	+0.83	–
	+1.10	0.92
$[Mn(slfh)(py)_2]\cdot 2H_2O$ (**2**)	-0.26	-0.50
	+0.83	–
	+1.103	+ 0.91
$[Mn(slfh)(2\text{-}pic)_2]\cdot 2H_2O$ (**3**)	-0.26	-0.50
	+0.83	–
	+1.03	+0.93

Antibacterial study: A clear inhibition zone had been observed near the agar well in the plates, which indicated the limited growth of the microorganisms. The free ligand and its Mn(IV) complexes showed moderate to high antibacterial activity against most of the tested Gram-negative and Gram-positive bacteria. Among the five complexes, complex **7** has shown high antibacterial activity against all the tested bacteria *Staphylococcus epidermis*, *Bacillus cerus*, *Klebsiella pneumonia*, *Escherichia coli*, *Enterobacter aerogenes* and *Proteus vulgaris* (Table-6). Complex **2** exhibited potent antibacterial activity against all the tested Gram-positive and Gram-negative bacteria except for *E. coli* [16,19,30].

The inhibition zone of 6-8 mm observed for ligand $slfhH_4$ against *Staphylococcus epidermis* (MTCC 435), *Enterobacter aerogenes* (MTCC 8559) and *Proteus vulgaris* (MTCC 426) indicated its modest activity while it is found to be highly active against *Escherichia coli* (MTCC 1669) with an inhibition zone of 10 mm. Metal complexes **1**, **2**, **3**, **4** and **7** that were screened for the antibacterial activity showed the zone of inhibition values in the range 6-20 mm, thus exhibiting higher activity against both Gram-positive and Gram-negative bacteria than the uncoordinated ligand [32].

Notably the microorganisms of Gram-negative nature, are known to be resistant to antimicrobial agent and hence, are

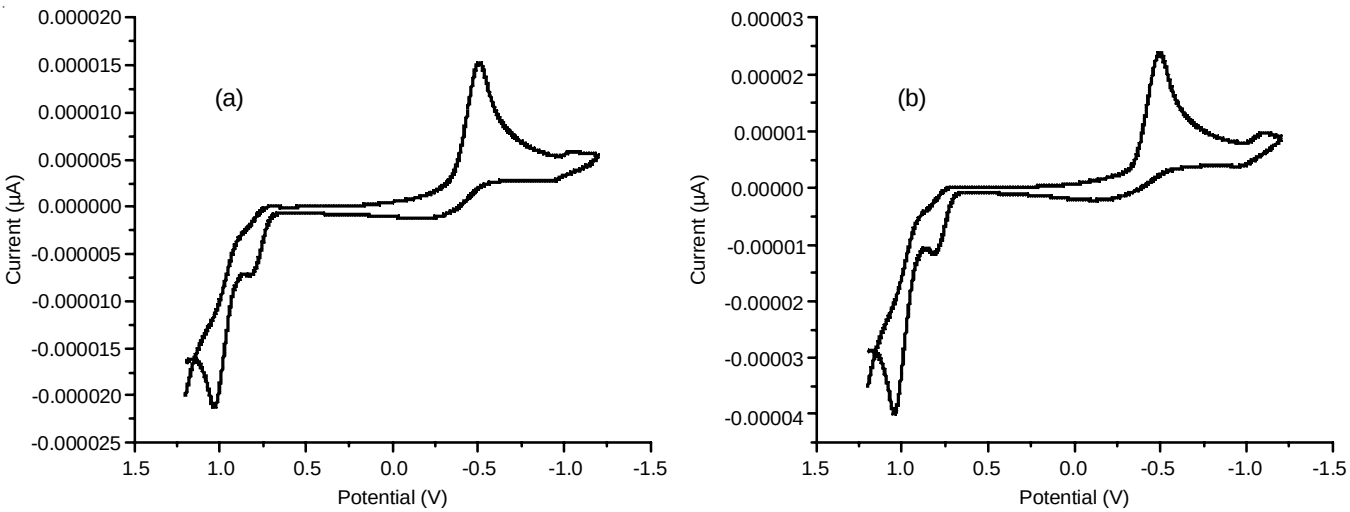

Fig. 4. Cyclic voltammograms of (a) ligand $slfhH_4$ and (b) complex $[Mn^{IV}(slfh)(py)_2]\cdot 2H_2O$ (**2**)

TABLE-6
ANTIMICROBIAL STUDIES OF THE LIGAND slfhH_4 AND ITS MANGANESE(IV) COMPLEXES

Schiff base/ Complexes	Zone of inhibition (mm)					
	Gram-positive		Gram-negative			
	Staphylococcus epidermis MTCC-435	*Bacillus cereus* MTCC-1305	*Klebsiella pneumonia* MTCC-10309	*Escherichia coli* MTCC-1669	*Enterobacter aerogenes* MTCC-8559	*Proteus vulgaris* MTCC-426
Ligand	08^{++}	–	-	10^{+++}	06^{++}	08^{++}
1	10^{+++}	08^{++}	10^{+++}	–	12^{+++}	–
2	10^{+++}	12^{+++}	14^{+++}	–	18^{+++}	10^{++}
3	–	–	10^{++}	–	16^{+++}	10^{+++}
4	–	08^{++}	19^{+++}	–	16^{+++}	–
7	14^{+++}	18^{+++}	20^{+++}	12^{+++}	18^{+++}	20^{+++}

Highly active = +++ (inhibition zone > 8.2 mm); moderately active = ++ (inhibition zone > 5.0-8.2); slightly active = + (inhibition zone > 2.5-5.0 mm); Inactive = – (inhibition zone < 2.5 mm)

difficult to treat [34,35]. The antibiotics that affect the Gram-negative bacteria may have potentials to act as antitumour drugs since researchers working in the field of antitimours, consider antimicrobial activity against the Gram-negative bacteria for preliminary tests as reported by Abdallah *et al*. [33]. Hence, these manganese(IV) complexes might be considered good in line for analysis on their antitumour activity and therefore would needed to be studied further.

Conclusion

The structural investigations of manganese(IV) complexes derived from disalicylaldehyde fumaroyldihydrazone under the set experimental conditions were studied. The structure of the ligand and its manganese(IV) complexes were confirmed by using elemental analysis, molar conductivity, thermal, magnetic moment studies along with mass, UV-Vis, ESR and IR spectroscopy. The magnetic moment data and ESR spectral studies revealed the presence of manganese in +4 oxidation state. The electronic spectral studies suggest the probable existence of octahedral stereochemistry around the Mn(IV) center. It is evident from IR studies that dihydrazone functions as a tetradentate ligand coordinating through NNOO donor sites. Further from the IR studies, it is proposed that in complexes **1-5**, the dihydrazone coordinates through azomethine nitrogens and phenolate oxygens to the Mn(IV) center, which occupy the equatorial positions while the axial positions remain occupied by donors like water/pyridine/2-picoline/3-picoline/4-picoline. In complexes **6** and **7**, azomethine nitrogens from dihydrazone and 2,2′-bipyridine (bpy) or 1,10-phenanthroline (phen) occupy the equatorial positions while phenolate oxygens are present in axial positions. The enolate oxygens do not coordinate metal center and the dihydrazone remains in enol form in all complexes. The crowding around manganese center due to various donor atoms probably leads to anti-*cis* configuration as suggested by the IR studies. The absence of metal-centered reductive and oxidative peaks in electrochemical data suggests the occurrence of the redox cycles in the voltammograms is only due to the existence of ligand-centered redox activity. The antibacterial studies showed that the free ligand showed moderate antibacterial activity against both Gram-negative and Gram-positive bacteria, while the Mn(IV) complexes showed higher activity against most Gram-negative and Gram-positive bacteria than the free ligand.

ACKNOWLEDGEMENTS

The authors acknowledge their gratitude for Prof. R.A. Lal, Department of Chemistry, North-Eastern Hill University, Shillong and Prof. V. Manivannan, Department of Chemistry, IIT Guwahati, Guwahati for continuous advice and discussions. The authors are also thankful to The Head, Department of Chemistry, Gauhati University, Guwahati for electrochemical studies and magnetic susceptibility; The Head, CIF, IIT Guwahati, Assam, India for elemental analysis data and EPR spectra, the Head, IASST, Boragaon, Guwahati, India for mass spectra. Two of the authors, PM and PS, also thank MHRD, Government of India for RA offered under the TEQIP-III project.

CONFLICT OF INTEREST

The authors declare that there is no conflict of interests regarding the publication of this article.

REFERENCES

1. A. Pui, *Croat. Chem. Acta*, **75**, 165 (2002).
2. A.D. Garnovskii, A.L. Nivorozhkin and V.I. Minkin, *Coord. Chem. Rev.*, **126**, 1 (1993); https://doi.org/10.1016/0010-8545(93)85032-Y
3. F.B. Dwyer, E. Mayhew, E.M.F. Roe and A. Shulman, *Br. J. Cancer*, **19**, 195 (1965); https://doi.org/10.1038/bjc.1965.24
4. X.M. Ouyang, B.L. Fei, T.A. Okamuro, W.Y. Sun, W.X. Tang and N. Ueyama, *Chem. Lett.*, **31**, 362 (2002); https://doi.org/10.1246/cl.2002.362
5. N. Raman, Y.P. Raja and A. Kulandaisamy, *Proc. Indiana Acad. Sci.*, **113**, 183 (2001); https://doi.org/10.1007/BF02704068
6. C. Jayabalakrishnan and K. Natarajan, *Transition Met. Chem.*, **27**, 75 (2002); https://doi.org/10.1023/A:1013437203247
7. M.K. Singh, N.K. Kar and R.A. Lal, *J. Coord. Chem.*, **62**, 1677 (2009); https://doi.org/10.1080/00958970802676649
8. F.A. El Saied, M.M. Abd-Elzaher, A.S. El Tabl, M.M.E. Shakdofa and A.J. Rasras, *Beni Suef Univ. J. Basic Appl. Sci.*, **6**, 24 (2017); https://doi.org/10.1016/j.bjbas.2016.12.005
9. A.I. Vogel, Text Book of Quantitative Inorganic Analysis, ELBS and Longmans: London Ed. 4 (1978).
10. D. Basumatary, R.A. Lal and A. Kumar, *J. Mol. Struct.*, **1092**, 122 (2015); https://doi.org/10.1016/j.molstruc.2015.02.070
11. R.A. Lal, D. Basumatary, A.K. De and A. Kumar, *Transition Met. Chem.*, **32**, 481 (2007); https://doi.org/10.1007/s11243-007-0189-3

12. K.K. Narang and V. P. Singh, *Transition Met. Chem.*, **18**, 287 (1993); https://doi.org/10.1007/BF00207948
13. M. Sharma, K. Chauhan, R.K. Srivastava, S.V. Singh, K. Srivastava, J.K. Saxena, S.K. Puri and P.M.S. Chauhan, *Chem. Biol. Drug Des.*, **84**, 175 (2014); https://doi.org/10.1111/cbdd.12289
14. S. Carvalho, E. da Silva, R. Santa-Rita, S. de Castro and C. Fraga, *Bioorg. Med. Chem. Lett.*, **14**, 5967 (2004); https://doi.org/10.1016/j.bmcl.2004.10.007
15. D.P. Kessissoglou, X. Li, W.M. Butler and V.L. Pecoraro, *Inorg. Chem.*, **26**, 2487 (1987); https://doi.org/10.1021/ic00262a030
16. S.N. Shukla, P. Gaur, P. Vaidya, B. Chaurasia and S. Jhariya, *J. Coord. Chem.*, **71**, 3912 (2018); https://doi.org/10.1080/00958972.2018.1536267
17. T. Matsushita, L. Spencer and D.T. Sawyer, *Inorg. Chem.*, **27**, 1167 (1988); https://doi.org/10.1021/ic00280a016
18. Y. Gultneh, T.B. Yisgedu, Y.T. Tesema and R.J. Butcher, *Inorg. Chem.*, **42**, 1857 (2003); https://doi.org/10.1021/ic020131w
19. A. Harriman, *Coord. Chem. Rev.*, **28**, 147 (1979); https://doi.org/10.1016/S0010-8545(00)82012-3
20. R.A. Lal, S. Adhikari, A. Kumar, J. Chakraborty and S. Bhaumik, *Synth. React. Inorg. M. Chem.*, **32**, 81 (2002); https://doi.org/10.1081/SIM-120013148
21. R.A. Lal, D. Basumatary, O.B. Chanu, A. Lemtur, M. Asthana, A. Kumar and A.K. De, *J. Coord. Chem.*, **64**, 300 (2011); https://doi.org/10.1080/00958972.2010.542238
22. R. Pal, V. Kumar, A.K. Gupta, V. Beniwal and G.K. Gupta, *Med. Chem. Res.*, **23**, 4060 (2014); https://doi.org/10.1007/s00044-014-0986-0
23. A. Zülfikaroglu, Ç.Y. Ataol, E. Çglu, U. Çelikoglu and O. Idil, *J. Mol. Struct.*, 1199, 127012 (2020); https://doi.org/10.1016/j.molstruc.2019.127012
24. R.S. Joseyphus and M.S. Nair, *J. Coord. Chem.*, **62**, 319 (2009); https://doi.org/10.1080/00958970802236048
25. R. Bikas, M. Ghorbanloo, R. Sasani, P. Ingo and M. Gerd, *J. Coord. Chem.*, **70**, 819 (2017); https://doi.org/10.1080/00958972.2017.1281918
26. R. Mukhopadhyay, S. Bhattacharjee and R. Bhattacharyya, *J. Chem. Soc. Dalton Trans.*, 2799 (1994); https://doi.org/10.1039/DT9940002799
27. A.B.P. Lever, Inorganic Electronic Spectroscopy, Elsevier: New York, Amsterdam, Ed. 2 (1984).
28. V.P. Singh, P. Gupta and N. Lal, *Russ. J. Coord. Chem.*, **34**, 270 (2008); https://doi.org/10.1134/S1070328408040064
29. P.J. Chirik and K. Wieghardt, *Science*, **327**, 794 (2010); https://doi.org/10.1126/science.1183281
30. C.G. Efthymiou, V. Nastopoulos, C. Raptopoulou, A. Tasiopoulos, S. P. Perlepes and C. Papatriantafyllopoulou, *Bioinorg. Chem. Appl.*, **2010**, 960571 (2010); https://doi.org/10.1155/2010/960571
31. M.D. Ward and J.A. McCleverty, *J. Chem. Soc.*, 275 (2002); https://doi.org/10.1039/B110131P
32. P. Mahanta, P. Sarma, D. Basumatary and C. Medhi, *Res. J. Chem. Environ.*, **25**, 1 (2021).
33. M.S. Abdallah, M.A. Zayed and G.G. Mohamed, *Arab. J. Chem.*, **3**, 103 (2010); https://doi.org/10.1016/j.arabjc.2010.02.006
34. J.T.P. Matshwele, F. Nareetsile, D. Mapolelo, P. Matshameko, M. Leteane, D.O. Nkwe and S. Odisitse, *J. Chem.*, **2020**, 2150419 (2020); https://doi.org/10.1155/2020/2150419
35. H. Nikaido and T. Nakae, *Adv. Microb. Physiol.*, **20**, 163 (1980); https://doi.org/10.1016/S0065-2911(08)60208-8